Macromolecules
ARTICLE

Macromolecules **2011**, *44*, 993–998 **993**
DOI: 10.1021/ma102572s

Adjacent UCST Phase Behavior in Aqueous Solutions of Poly(vinyl methyl ether): Detection of a Narrow Low Temperature UCST in the Lower Concentration Range

Guy Van Assche,*,† Bruno Van Mele,† Ting Li,‡ and Erik Nies*,‡,§

†*Department of Physical Chemistry and Polymer Science, Vrije Universiteit Brussel, Belgium,* ‡*Polymer Research Division, Department of Chemistry, The Leuven Mathematical Modeling and Computational Science Centre (LMCC) and the Leuven Materials Research Centre (LMRC), Katholieke Universiteit Leuven, Celestijnenlaan 200F, B-3001 Heverlee, Belgium, and* §*Laboratory of Polymer Technology, Eindhoven University of Technology, The Netherlands*

Received November 10, 2010; Revised Manuscript Received December 21, 2010

ABSTRACT: We provide the first experimental evidence for the existence of a low concentration narrow UCST miscibility gap, which is the second of two narrow miscibility gaps constituting together adjacent UCST phase behavior. The existence of adjacent UCST miscibility phase behavior in aqueous polymer solutions has been theoretically predicted, but so far escaped experimental verification. We have been able to determine the low concentration narrow UCST miscibility gaps from the changes in apparent heat capacity observed in stepwise isothermal cooling modulated temperature differential scanning calorimetry (MTDSC) experiments. In wide-angle X-ray diffraction (WAXD) experiments it was unambiguously demonstrated that the MTDSC heat capacity changes are not due to crystallization. Together with earlier experimental results on the high concentration narrow UCST miscibility gap, the bimodal LCST miscibility gap and the sigmoidal melting line of ice the experimental results reported in this work complete the full experimental verification of the predicted complex phase behavior of aqueous solutions of PVME. As far as the authors are aware, this is the first system where adjacent UCST phase behavior is found. On the basis of the theoretical predictions the observed phase behavior could be more general and other systems may exist where similar behavior can be observed.

Introduction

In the earliest papers drawing attention to the peculiar bimodal lower critical solution (LCST) phase behavior of aqueous PVME solutions the influence of quench depth and viscoelasticity on the phase separation process taking place upon entering the LCST miscibility gap was studied[1−5] Later Koningsveld, Solc, Berghmans, and co-workers showed that the bimodal phase behavior was a true thermodynamic transition, fitting in a more generic phenomenological framework for the phase behavior of polymer solutions and mixtures.[6] In particular it was shown that the phase behavior of water-soluble polymers may deviate from our common understanding, embodied in the Flory−Huggins (FH) theory.[7,8] According to this latter theory, the occurrence of miscibility gaps is dominated by the balance of the dispersive interactions and the combinatorial entropy in such a way that with increasing polymer chain length miscibility gaps become more asymmetric and the liquid−liquid (LL) critical point moves to lower polymer concentration. Moreover, in the limit of an infinitely long polymer in solution, the LL critical point is located at infinite dilution and the critical temperature coincides with the Θ-temperature of the polymer/solvent system.[9,10] Many but not all polymer systems obey these principles and in particular aqueous polymer solutions may deviate from them. For instance aqueous solutions of poly(vinyl caprolactam) (PVCL)[11,12] and poly(2-isopropyl-2-oxazoline) (PIPOZ)[13] show classic FH behavior as discussed above, but aqueous solutions of poly(*N*-isopropylacrylamide) (PNiPA) behave very differently.[14,15] For this polymer it has been shown experimentally that the critical composition does not vary significantly with molar mass (including the repeating unit of the polymer, i.e. N-(isopropyl) propionamide (NiPPA)) and is about equal to $w_{PNiPA} \cong 0.5$.[14,16] Another remarkable result is obtained for poly(vinyl methyl ether) (PVME) in water that shows bimodal phase behavior with the LCST miscibility gap having 2 stable critical points: one changing with molar mass as predicted by the FH theory and a second critical point at high polymer concentrations that does not vary significantly with polymer molar mass.[6,15,17−20]

The occurrence of LCST phase behavior in these aqueous polymer solutions is not really surprising and is characteristic of polymer solutions that exhibit hydrogen bonding[21−23]and numerous experimental, theoretical and simulation studies concerning the importance of hydrogen bond interactions for the observed properties of this class of polymer systems are available. (Modulated temperature) differential scanning calorimetry ((MT)-DSC), infrared (IR), nuclear magnetic resonance (NMR), dielectric, microwave and ultrasonic spectroscopy, scattering, and diffraction methods are frequently used experimental techniques to study the phase behavior of polymer solutions and the statics and dynamics of the hydrogen bond interactions. Molecular simulations methods were used to investigate the dynamics and structure of hydrogen bonds in detail.[24−28]

It is also recurrently suggested that phase behavior of these flexible synthetic polymers in solution has similarities to the denaturation of proteins in which the hydration layer of the protein plays an important role and numerous studies are

*Corresponding authors. E-mail: (G.V.A.) gvassche@vub.ac.be; (E.N.) Erik.Nies@chem.kuleuven.be.

Published on Web 01/21/2011

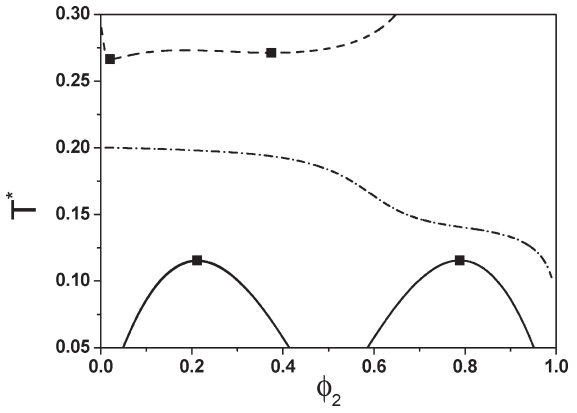

Figure 1. Theoretically predicted temperature−composition ($T^*-\phi_2$) phase diagram of a model polymer solution including between solvent−solvent and solvent−polymer association interactions as predicted by the lattice Wertheim perturbation theory. Predicted bimodal LCST spinodal curve (dashed, ---), melting line of the solvent (dash-dotted, -·-); adjacent UCST's spinodals (solid, —) and critical conditions (■) (after ref 20). T^* is the reduced temperature, and ϕ_2 is the volume fraction of polymer in the solution.

available on the hydration of synthetic polymers as a function of molecular and thermodynamic parameters.

In the case of aqueous solutions of PVME the influence on the phase behavior and the hydration of the polymer were investigated as a function of temperature, pressure, type of solvent, solvent mixtures, the addition of salts and different end groups.[29−38] In several studies the hydration of PVME is interpreted in terms of different types of water (free water, bound water, and freezable and nonfreezable water) in phase-separated solutions as well as in homogeneous solutions in the vicinity of the LCST miscibility gap.[39−47] Connected to this the existence of specific complexes between PVME and water in solution has been suggested and investigated.[48−54] Also scattering techniques (in particular neutron scattering) were used to characterize the interactions between water and the polymer.[19,20,55]

All these studies provide a wealth of detailed information but did not succeed in explaining the precise relationship between the hydrogen bonding and other molecular interactions and the peculiar phase behavior.

Improved theoretical understanding of the peculiar bimodal phase behavior of PVME/water was obtained by taking into account the effects of hydrogen bonding interactions on the thermodynamics of polymer solutions. Employing a lattice version of the Wertheim theory for saturation interactions, the bimodal LCST phase behavior and the dependence on molar mass as seen in PVME/water was predicted (see Figure 1, dashed line).[20,56] More importantly, the bimodal LCST was not the only intriguing theoretical prediction for the PVME/water phase behavior. It was predicted that below the LCST miscibility gap, the system should have two narrow adjacent UCST miscibility gaps, depicted in Figure 1 by the solid curves.[20] Finally, combined with the standard thermodynamic model for the solid state of water (ice) it was predicted that water should have a sigmoidal melting line spanning the entire concentration range (see Figure 1, dash-dotted line).[20,56]

Stimulated by these theoretical results, dedicated experiments were conducted to investigate these nontrivial predictions for the PVME/water system. Using small angle neutron scattering (SANS) the bimodal phase behavior was also observed in PVME20/D_2O.[19,20] In addition the SANS experiments (1) provided the direct experimental proof of the existence of a narrow UCST spinodal at high polymer concentrations in agreement with the theoretical predictions and (2) provided direct experimental evidence that a true complex between water and polymer is not formed in the conditions used in the experiment.[20] The PVME20 sample used in these experiments is identical to the one used in this work (see Experimental Section). Using MTDSC evidence was provided of the existence of the bimodal LCST, and also of the UCST gap at high polymer concentration for another PVME sample in H_2O (the PVME sample used in these experiments, PVME4, had a number-average molar mass M_n = 4 kg mol^{-1} and M_w/M_n = 1.10).[56] The presence of the narrow UCST at high polymer concentrations was supported (1) through quasi-isothermal heat capacity measurements in stepwise cooling experiments, in which the creation of coexisting phases in a liquid−liquid phase separation introduces time-dependencies in the apparent specific heat capacity, and (2) by accurate measurements of the glass transition temperatures, which split in two transitions after phase separation. From the latter results a reasonably accurate estimate of the composition of the coexisting phases was obtained, confirming the narrowness of the observed UCST miscibility gap. Finally, in in situ FTIR and DSC experiments the existence of the sigmoidally shaped melting line of water was also confirmed for PVME4 and PVME20 in H_2O[56,57] The above-mentioned experimental data on the phase behavior of PVME20/(D_2O or H_2O) are collected in Figure 3b, where they are brought together with the experimental results obtained in this work.

So far, from all the theoretical predictions only the existence of a narrow UCST gap at low polymer concentration was not yet confirmed by experiment.

For the higher polymer concentrations ($w_{PVME} \geq 0.5$) used in the SANS, IR and DSC experiments, it was relatively easy to study liquid mixtures even below the equilibrium liquid−solid transition line of water. In aqueous PVME mixtures a typical supercooling of ca. 25 K is needed to induce nucleation and crystallization of water in DSC experiments at a cooling rate of 1 K/min. As a result of the sigmoidal melting line, the concentrated mixtures are close to their glass transition temperature at these considerable supercoolings, so that nucleation and crystallization rates are significantly decreased, making the study of liquid mixtures below the equilibrium melting line possible.

For the lower polymer concentrations, the gap between the melting line and the glass transition line is much larger and at a supercooling of 25 K nucleation and crystallization proceed fast, making it much more difficult to observe the phase behavior of the liquid solutions at these sub ambient conditions. However, based on the theoretical predictions and the actual temperature range of the high concentration UCST, we may hope that also the narrow low concentration UCST could be located at a smaller supercooling, where the nucleation and crystallization rates are sufficiently low so that that the liquid−liquid UCST miscibility gap can still be observed under proper experimental conditions.

In this paper, we therefore study in more detail the properties of aqueous solutions of PVME for lower concentrations ($w_{PVME} < 0.5$), at smaller supercoolings where nucleation and crystallization rates for crystallization are sufficiently small, with the aim to find evidence of the narrow low temperature UCST phase behavior at low polymer concentrations.

Experimental Section

Materials. Poly(vinyl methyl ether) (PVME20) dissolved in water (mass fraction PVME, w_{PVME} = 0.5) was purchased from Aldrich Chemical Co. Inc. (mass average molar mass, M_w = 20 kg mol^{-1}, determined from SANS;[19] polydispersity, M_w/M_n = 2.5, derived from size exclusion chromatography).

A series of PVME/water solutions with varying polymer concentration was obtained directly from the w_{PVME} = 0.5 solution (as received from Aldrich) by adding the proper amount of water. The concentration of all solutions was

controlled by thermogravimetric analysis (TA Instruments TGA 2950).

Differential Scanning Calorimetry. The modulated temperature differential scanning calorimetry (MTDSC) measurements were performed on a TA Instruments Q1000 T-zero DSC equipped with a refrigerated cooling system (RCS-90) and a nitrogen purge. In a Q1000 system, the underlying temperature and temperature amplitude are remarkably stable (within ±0.002 °C and ±0.0001 °C, respectively, for 1000 min).

A T-zero-calibration procedure (type T4) was performed. The determination of the thermal capacitances and resistances comprises the measurement of the instrument baseline with empty sensors, followed by a measurement with sapphire disks directly on sample and reference sensors. Subsequently indium is used for fine-tuning the temperature and enthalpy calibration. No additional calibration was performed for the heat capacity.

Standard temperature modulation conditions were employed with amplitude A_T of 0.50K and a period p of 60 s. Nonisothermal experiments were performed at an underlying heating rate of 1 K.min^{-1} unless stated otherwise. Stepwise quasi-isothermal cooling experiments were performed starting from solutions homogenized at 20 °C using steps of −3 K of at least 400 min until phase separation or crystallization occurred. Subsequently the sample is reheated at 1 K/min to 20 °C. Samples of 1 to 10 mg were introduced in hermetic aluminum crucibles.

Wide-Angle X-ray Diffraction. Isothermal time-resolved wide-angle X-ray diffraction (WAXD) experiments up to 180 min were carried out at the Dutch−Belgian beamline (DUBBLE, BM26-B) of the European Synchrotron Radiation Facility (ESRF, Grenoble, France).[58] Data were collected using an X-ray wavelength, λ, of 1.1 Å on a two-dimensional CCD-X-ray digital camera, VHR (2657 × 3955 pixels) from Photonic Science. The diffraction peaks of a HDPE secondary standard and of a crystalline Si standard were used to calibrate scattering angles. The image plate inclination angles were calibrated using a crystalline Si standard and the 2D scattering data were azimuthally integrated. The background scattering due to the experimental setup and the sample holder was not subtracted as we are only interested in the qualitative analysis, i.e. the absence or presence of ice diffraction peaks. The samples were enclosed in the same aluminum crucibles used for the DSC measurements and placed in a Linkam hot stage for temperature control between −30 and +20 °C. During the isothermal measurement 2D diffraction patterns were accumulated and stored every 12 s until crystallization was observed or up to the longest measurement time.

WAXD experiments for longer isothermal times were collected with a Bruker-AXS diffractometer using CuKα (wavelength λ, of 1.54 Å) and equipped with a 2D CCD detector (SMART 6000) cooled to −57 °C to reduce background noise. Scattering angles were calibrated using silver behenate.

Samples were contained in thin wall quartz capillaries (diameter 0.5 mm and 1 mm, Glass, Germany) and 2D diffraction patterns were accumulated and stored every minute. In these longer duration WAXD experiments the same temperature−time program was followed as in the isothermal MTDSC experiments.

In both WAXD setups the sample to detector distance was chosen to detect d-spacings in the range [4.0 Å − 1.9 Å] covering the 100 (d = 3.897 Å), 002 (d = 3.669 Å), 101 (d = 3.440 Å), 102 (d = 2.671 Å), 110 (d = 2.489 Å), 103 (d = 2.071 Å), 200 (d = 1.947 Å), 112 (d = 1.917 Å) and 201 (d = 1.883 Å) lattice reflections of hexagonal ice.[59]

Results and Discussion

1.1. Nonisothermal Crystallization and Melting of Water. The onset of crystallization was measured for a series of aqueous PVME solutions by standard DSC at 1 K/min. When cooling down a w_{PVME} = 0.30 mixture, for example, crystallization of water starts near −25 °C (see Figure 2). By comparison with the subsequent melting in heating, it can be seen that a supercooling of ca. 25 K is needed to induce nucleation and crystallization. The crystallization process intrinsically goes hand-in-hand with a phase separation between ice-crystals and a PVME-rich phase that subsequently vitrifies upon further cooling. Once nucleation has occurred, the subsequent crystallization process is very fast: it takes only a few seconds (ca. 10 s for a solution with w_{PVME} = 0.30). This type of crystallization behavior is typically observed in nonisothermal experiments for polymer solutions below w_{PVME} = 0.40.

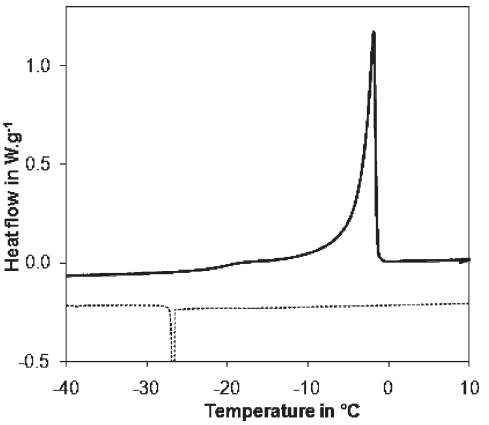

Figure 2. Heat flow during nonisothermal cooling (thin dashed line) and subsequent heating (thick solid line) of an aqueous PVME solution with w_{PVME} = 0.3 measured in the standard DSC mode. The crystallization peak is not fully shown.

During heating a double or bimodal melting endotherm is observed. The bimodal melting endotherms are quantitatively related to the shape of the sigmoidal shape of the melting line that was predicted theoretically and observed experimentally.[20,56,57] The crystallization temperatures determined from the nonisothermal DSC experiments in the concentration range 0 < w_{PVME} < 0.5 are shown in Figure 3a (◆). In Figure 3a we also show the experimental melting temperatures (●) obtained from the nonisothermal DSC experiments. In Figure 3b we compare the melting temperatures from this work to the bimodal melting line (○) obtained by Loozen et al.[57] Excellent agreement between literature and our data is seen.

The very fast crystallization of water at temperatures around −20 to −25 °C upon cooling aqueous PVME solutions with w_{PVME} < 0.5 complicates the study of the possible low temperature UCST demixing for these solutions, which is theoretically predicted to occur at similar temperatures as the UCST at higher concentrations (see Figure 1). Indeed, the glass transition based method used in[56] to detect the low temperature UCST at high concentration (w_{PVME} > 0.5), cannot be used to detect UCST-type phase separation in the low polymer concentration region, as crystallization of water occurs before the glass transition is reached. Therefore, indications of the presence of UCST demixing where searched for using quasi-isothermal heat capacity measurements in stepwise cooling, a method also used previously to detect the low temperature UCST at high concentrations.

1.2. UCST Demixing in PVME/Water at Low Temperatures and Low Polymer Concentrations. *MTDSC Results.* Quasi-isothermal heat capacity measurements in a stepwise cooling experiment (steps −3 K) are illustrated in Figure 4 for a w_{PVME} = 0.30 PVME20/water mixture. The measured apparent specific heat capacity, c_p^{app}, shows a gradual

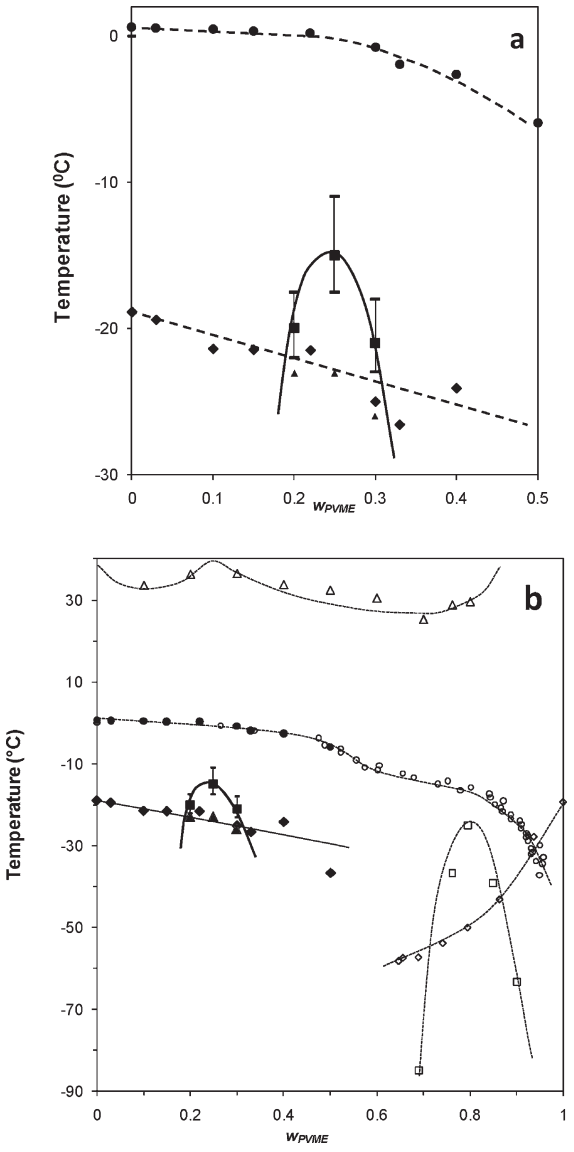

Figure 3. (a) Low concentration narrow UCST miscibility gap obtained by quasi-isothermal MTDSC experiments: temperatures where the strongest increase of c_p^{app} is observed (■); vertical bars indicate the region of temperature where c_p^{app} increases, crystallization curve for PVME20 from heat flow measurements during nonisothermal cooling (◆) and from WAXD (▲), melting line from this work (●). (b) Temperature−composition phase diagram of PVME/water: bimodal LCST miscibility gap determined by SANS in D_2O (Δ)[20] melting line of water from Loozen et al. (○)[57] and from this work (●); crystallization curve for PVME20 from heat flow measurements during nonisothermal cooling (◆) and from WAXD (▲); T_g-composition curve of PVME water mixtures (◇);[17] high concentration narrow UCST miscibility gap (□).[20] Lines are drawn to guide the eye.

increase of c_p^{app} with time at −21 °C, which can be attributed to the development of an excess heat capacity contribution, c_p^{excess}, resulting from a slow phase separation process. In fact, analysis of the c_p^{app} data of the individual quasi-isothermal sections shows that a statistically significant positive slope is already observed at −18 °C. The presence of an excess heat capacity resulting from (reversible) demixing and remixing induced by the temperature modulation was evidenced before in polymer−water solutions,[18,56,60] hydrogels,[61] and polymer blends.[62,63] The gradual increase in c_p^{excess} can be attributed to a gradual increase in the interfacial contact area between the coexisting phases.[56,64] Unfortunately, the observed slow increase of c_p^{app} does not

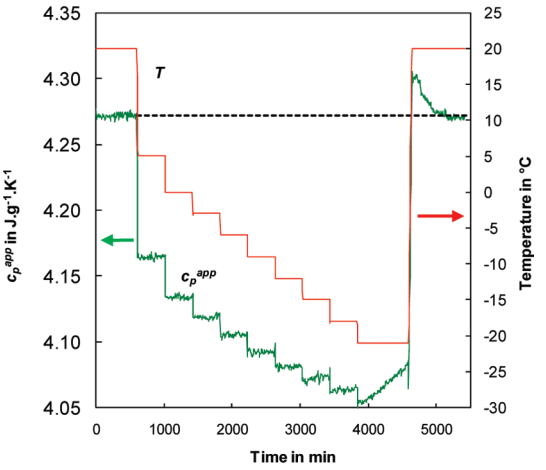

Figure 4. Time-evolution of c_p^{app} during stepwise quasi-isothermal measurements for w_{PVME} = 0.3 PVME/water in steps of 3 °C between 0 and −21 °C. UCST demixing at −21 °C is indicated by the increasing apparent heat capacity and by the decreasing apparent heat capacity during the subsequent remixing at 20 °C.

allow distinguishing between a nucleation and growth or spinodal decomposition (plus coarsening) mechanism.

The occurrence of phase separation upon cooling is further supported by the observation of remixing after reheating from −21 to +20 °C: at 20 °C c_p^{app} starts at a level above the value for the homogeneous solution, c_p^{base} (Figure 4, dashed line), and subsequently decreases toward c_p^{base}, as the c_p^{excess} contribution gradually diminishes due to the remixing of the sample. Both the phase separation process at −21 °C and the remixing at 20 °C are slow and similar to the time scales observed for phase separation at the high concentration UCST.[56] The absolute values of the increase and decrease of c_p^{app} at −21 and 20 °C, respectively, are quite similar. Note that the observed magnitude of c_p^{excess} during the UCST phase separation is about 100 times smaller than that observed in the LCST phase separation region,[56] but nevertheless clearly significant. It cannot be attributed to crystallization of water or vitrification, since both transformations would provoke a decrease of the specific heat capacity.[56] Moreover, the melting of ice is not observed during the subsequent heating.

The temperature at which c_p^{app} starts to increase with time was taken as the UCST-demixing temperature upon cooling. Similar patterns were observed for two other compositions, namely, w_{PVME} = 0.20 and w_{PVME} = 0.25 albeit at different temperatures. Using these results, the UCST demixing curve illustrated in Figure 3a was composed, with the solid squares (■) indicating the temperature where the increase in c_p^{app} is the strongest, and with the vertical bar representing the range in temperature where c_p^{app} increases significantly. The maximum temperature of −15 °C observed for the UCST at low concentration is comparable to that observed at the high concentration side (see Figure 3b), which is in satisfying agreement with the predictions. In the theoretical predictions the critical temperatures of the adjacent UCST's are identical which is related to the choice of the values of the different parameters in the theory.[20] In a more refined comparison of theory with experimental data, different values for the critical temperatures can be obtained by appropriate choice of the values of the theoretical parameters.[65]

Considering the evolution of the crystallization temperature measured upon cooling, one can expect that for compositions below w_{PVME} = 0.20 and above w_{PVME} = 0.30, the UCST-demixing cannot be observed as crystallization

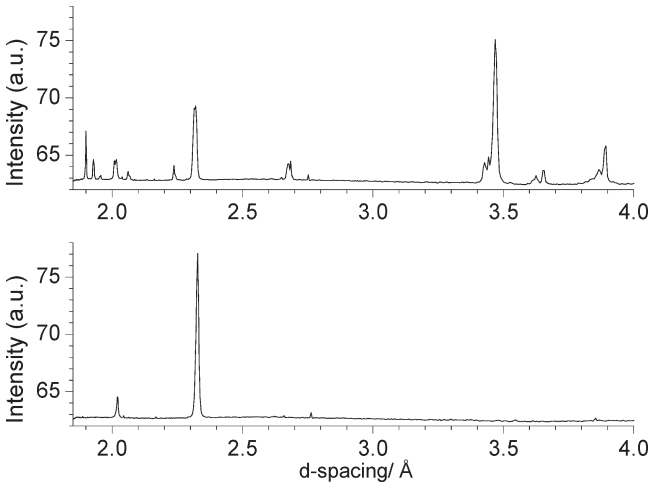

Figure 5. WAXD patterns for an aqueous PVME mixture with w_{PVME} = 0.2 at T = 25 °C (bottom panel) and T = −25 °C (top panel). *d*-spacings of 2.024 and 2.338 Å are from the Al crucible containing the sample, the other diffraction peaks in the top panel are due to ice (coming from the 100, 002, 101, 102, 110, 103, 200, 112, and 201 lattice reflections of hexagonal ice).[59]

Table 1. Summary of WAXD Results[a]

	w_{PVME}		
temperature	0.20	0.25	0.30
0 °C → −21 °C (steps 3 K)	×	×	×
−23 °C	∼77	∼173	×
−26 °C			∼138

[a] When no crystallization was observed in the isothermal segment of 400 min, this is denoted by (×); when crystallization has occurred in an isothermal time segment, the time to crystallization is given in minutes.

occurs first (crystallization temperature is higher than the expected UCST demixing temperature, see Figure 3a).

1.3. WAXD in PVME/Water at Low Temperatures and Low Polymer Concentrations. The objective of the WAXD experiments is to further ascertain by an independent technique that the heat capacity changes seen in the MTDSC experiments are not due to the crystallization of water. Crystallization in the aqueous PVME mixtures will show up in the WAXD patterns by prominent diffraction peaks related to the presence of ice.[48] WAXD patterns were recorded as a function of time during stepwise isothermal measurements for the same polymer concentrations as measured in the DSC experiments. At the DUBBLE synchrotron facility, stepwise isothermal measurements were done with a stepwise change in temperature (ΔT = 3K) every 180 min. At each temperature WAXD patterns were stored every 12 s and analyzed as explained in the Experimental Section. In these experiments, the samples contained in aluminum crucibles for DSC experiments were used.

Longer duration WAXD measurements were performed on a Bruker AXS SMART 6000 apparatus. In these experiments the samples were contained in thin wall quartz capillaries and the time−temperature program used in the MTDSC experiments was reproduced as closely as possible. In this way, one can use the WAXD data to detect the formation of ice in the solution during the isothermal experiments on the time scales relevant for the MTDSC experiments.

For a PVME/water mixture with composition w_{PVME} = 0.20, Figure 5 shows two typical diffraction patterns obtained after integration of the 2D diffraction patterns. The bottom panel in Figure 5 is taken at T = 25 °C, at which crystallization has not occurred, and the top panel in Figure 5 is taken at T = −25 °C, at which temperature crystallization of ice has occurred. Before crystallization we see in the diffraction pattern (bottom panel of Figure 5) 2 strong diffraction peaks due to the polycrystalline aluminum DSC crucible and corresponding to *d*-spacings of 2.338 and 2.024 Å.[66] At the lower temperature (top panel Figure 5) crystallization has occurred and we observe the 100, 002, 101, 102, 110, 103, 200, 112, and 201 lattice reflections of hexagonal ice.[59]

The WAXD results for all compositions and temperatures are summarized in Table 1. When crystallization occurred in a specific isothermal segment the time to crystallization is shown, when no crystallization was observed in the isothermal segment this is denoted by (×). The WAXD results confirm that the variations in the MTDSC heat capacity signal c_p^{app} are not due to crystallization. The approximate crystallization temperatures determined from the WAXD results are also shown in the phase diagram shown in Figure 3a (▲) and are in good agreement with the DSC results.

Conclusions

In the system PVME/water, highly nontrivial phase behavior was predicted. Most of these predictions were already verified. Specifically, the existence of bimodal LCST phase behavior at higher temperature, the existence of a sigmoidal melting line of water with polymer concentration, and the existence of a low temperature narrow UCST miscibility gap at high polymer concentrations were experimentally confirmed. Here we gave the first experimental evidence for the existence of the narrow low concentration UCST miscibility gap, which is the second of two miscibility gaps constituting together adjacent UCST phase behavior according to the theoretical predictions. It was possible to detect the low concentration narrow UCST miscibility gap by carefully controlling the supercooling in the solutions: at not too high supercoolings, the rate of nucleation and subsequent crystallization are strongly suppressed.

Particularly, changes in the apparent heat capacity from MTDSC upon stepwise isothermal cooling were related to the occurrence of UCST liquid−liquid demixing. The occurrence of phase separation upon cooling is further supported by the observation of remixing after reheating. From WAXD experiments, it was unambiguously demonstrated that the MTDSC heat capacity changes are not related to the occurrence of crystallization.

Together with the earlier experimental results on the high concentration narrow UCST miscibility gap, the bimodal LCST miscibility gap and the sigmoidal melting line of ice completes the experimental verification of the complex predicted phase behavior for aqueous solutions of PVME. As far as the authors are aware, this is the first system where this peculiar and highly nontrivial phase behavior is found. However, based on the theoretical predictions, the observed phase behavior could be more general and other systems may exist where similar behavior can be observed.

Acknowledgment. The authors thank the Research Foundation-Flanders (FWO Vlaanderen) for financial support. L.T. is indebted to the Katholieke Universiteit Leuven for a postdoctoral fellowship (OT 03/93). Prof. Luc Van Meervelt, Dr. Koen Robeyns, and Dr. Kristof Van Hecke of the department of Chemistry of the Katholieke Universiteit Leuven are acknowledged for the use of and assistance with the in house X-ray experiments. The authors gratefully acknowledge the staff of DUBBLE at the ESRF in France and dr. Filip Meersman of the department of Chemistry of the Katholieke Universiteit Leuven

for assisting in the WAXS measurements and FWO-Vlaanderen for supporting the DUBBLE project.

References and Notes

(1) Tanaka, H.; Nishi, T. *Jpn. J. Appl. Phys.* **1988**, *27*, L1783–L1786.
(2) Tanaka, H.; Nishi, T. *Jpn. J. Appl. Phys.* **1988**, *27*, L1787–L1790.
(3) Tanaka, H. *AIP Conf. Proc.* **1992**, *256*, 238.
(4) Tanaka, H. *Phys. Rev. E Stat. Nonlin. Soft Matter Phys.* **1995**, *51*, 1313–1329.
(5) Tanaka, H.; Nishi, T. In *Dynamics and patterns in complex fluids: new aspects of the physics-chemistry interface: proceedings of the 4th Nishinomiya-Yukawa Memorial Symposium, Nishinomiya City, Japan, October 26−27, 1989*; Springer-Verlag: Berlin, New York, 1990; p 119.
(6) Schafer-Soenen, H.; Moerkerke, R.; Berghmans, H.; Koningsveld, R.; Dusek, K.; Solc, K. *Macromolecules* **1997**, *30*, 410–416.
(7) Flory, P. J. *J. Chem. Phys.* **1941**, *9*, 660.
(8) Huggins, M. L. *J. Chem. Phys.* **1941**, *9*, 440.
(9) Rubinstein, M.; Colby, R. H. *Polymer Physics*; 1st ed.; Oxford University Press: New York, 2003.
(10) Flory, P. J. *Principles of Polymer Chemistry*; Cornell University Press: Ithaca, NY, 1953.
(11) Sun, T.; King, H. E. *Macromolecules* **1998**, *31*, 6383–6386.
(12) Meeussen, F.; Nies, E.; Berghmans, H.; Verbrugghe, S.; Goethals, E.; Du Prez, F. *Polymer* **2000**, *41*, 8597–8602.
(13) Zhao, J.; Hoogenboom, R.; Van Assche, G.; Van Mele, B. *Macromolecules* **2010**, *43*, 6853–6860.
(14) Afroze, F.; Nies, E.; Berghmans, H. *J. Mol. Struct.* **2000**, *554*, 55–68.
(15) Van Durme, K.; Van Assche, G.; Van Mele, B. *Macromolecules* **2004**, *37*, 9596–9605.
(16) Geukens, B.; Meersman, F.; Nies, E. *J. Phys. Chem. B* **2008**, *112*, 4474–4477.
(17) Meeussen, F.; Bauwens, Y.; Moerkerke, R.; Nies, E.; Berghmans, H. *Polymer* **2000**, *41*, 3737–3743.
(18) Swier, S.; Van Durme, K.; Van Mele, B. *J. Polym. Sci. B Polym. Phys.* **2003**, *41*, 1824–1836.
(19) Nies, E.; Ramzi, A.; Berghmans, H.; Li, T.; Heenan, R. K.; King, S. M. *Macromolecules* **2005**, *38*, 915–924.
(20) Nies, E.; Li, T.; Berghmans, H.; Heenan, R. K.; King, S. M. *J. Phys. Chem. B* **2006**, *110*, 5321–5329.
(21) Walker, J. S.; Vause, C. A. *Phys. Lett. A.* **1980**, *79*, 421–424.
(22) Panayiotou, C.; Sanchez, I. C. *J. Phys. Chem.* **1991**, *95*, 10090–10097.
(23) Dormidontova, E. E. *Macromolecules* **2002**, *35*, 987–1001.
(24) Wu, R. L.; Ji, Q.; Kong, B.; Yang, X. Z. *Sci. China Ser. B: Chem.* **2008**, *51*, 736–742.
(25) Zeng, X.; Yang, X. *J. Phys. Chem. B* **2004**, *108*, 17384–17392.
(26) Tamai, Y.; Tanaka, H.; Nakanishi, K. *Mol. Simul.* **1996**, *16*, 359–374.
(27) Tamai, Y.; Tanaka, H.; Nakanishi, K. *Macromolecules* **1996**, *29*, 6750–6760.
(28) Tamai, Y.; Tanaka, H.; Nakanishi, K. *Macromolecules* **1996**, *29*, 6761–6769.
(29) Horne, R. A.; Almeida, J. P.; Day, A. F.; Yu, N. T. *J. Colloid Interface Sci.* **1971**, *35*, 77–84.
(30) Loozen, E.; Nies, E.; Heremans, K.; Berghmans, H. *J. Phys. Chem. B* **2006**, *110*, 7793–7802.
(31) Van Durme, K.; Van Mele, B.; Bernaerts, K. V.; Verdonck, B.; Du Prez, F. E. *J. Polym. Sci. B Polym. Phys.* **2006**, *44*, 461–469.
(32) Van Durme, K.; Van Assche, G.; Rahier, H.; Van Mele, B. *J. Therm. Anal. Calorim.* **2009**, *98*, 495–505.
(33) Van Durme, K.; Rahier, H.; Van Mele, B. *Macromolecules* **2005**, *38*, 10155–10163.
(34) Bergé; Koningsveld, R.; Berghmans, H. *Macromolecules* **2004**, *37*, 8082–8090.
(35) Maeda, Y. *Langmuir* **2001**, *17*, 1737–1742.
(36) Maeda, Y.; Yamamoto, H.; Ikeda, I. *Macromol. Rapid Commun.* **2004**, *25*, 720–723.
(37) Kaatze, U. *Prog. Colloid Polym. Sci.* **1978**, 214–224.
(38) Kaatze, U.; Gottmann, O.; Podbielski, R.; Pottel, R.; Terveer, U. *J. Phys. Chem.* **1978**, *82*, 112–120.
(39) Guan, L.; Xu, H.; Huang, D. *Polym. J.* **2010**, *42*, 540–545.
(40) Guo, Y.; Peng, Y.; Wu, P. *J. Mol. Struct.* **2008**, *875*, 486–492.
(41) Shinyashiki, N.; Shimomura, M.; Ushiyama, T.; Miyagawa, T.; Yagihara, S. *J. Phys. Chem. B* **2007**, *111*, 10079–10087.
(42) Spěváček, J.; Hanyková, L. *Macromolecules* **2005**, *38*, 9187–9191.
(43) Cerveny, S.; Colmenero, J.; Alegria, A. *Macromolecules* **2005**, *38*, 7056–7063.
(44) Spěváček, J.; Hanyková, L.; Starovoytova, L. *Macromolecules* **2004**, *37*, 7710–7718.
(45) Shinyashiki, N.; Yagihara, S.; Arita, I.; Mashimo, S. *J. Phys. Chem. B* **1998**, *102*, 3249–3251.
(46) Spěváček, J.; Hanyková, L. *Macromol. Symp.* **2007**, *251*, 72–80.
(47) Spěváček, J.; Starovoytova, L.; Hanyková, L.; Kouřilová, H. *Macromol. Symp.* **2008**, *273*, 17–24.
(48) Zhang, J.; Bergé, B.; Meeussen, F.; Nies, E.; Berghmans, H.; Shen, D. *Macromolecules* **2003**, *36*, 9145–9153.
(49) Zhang, T.; Li, T.; Nies, E.; Berghmans, H.; Ge, L. *Polymer* **2009**, *50*, 1206–1213.
(50) Zhang, J. M.; Zhang, G. B.; Wang, J. J.; Lu, Y. L.; Shen, D. Y. *J. Polym. Sci., B: Polym. Phys.* **2002**, *40*, 2772–2779.
(51) Zhang, J.; Teng, H.; Zhou, X.; Shen, D. *Polym. Bull.* **2002**, *48*, 277–282.
(52) Meeussen, F.; Bauwens, Y.; Moerkerke, R.; Nies, E.; Berghmans, H. *Polymer* **2000**, *41*, 3737–3743.
(53) Maeda, H. *J. Polym. Sci. B Polym. Phys.* **1994**, *32*, 91–97.
(54) Van Durme, K.; Loozen, E.; Nies, E.; Van Mele, B. *Macromolecules* **2005**, *38*, 10234–10243.
(55) Okano, K.; Takada, M.; Kurita, K.; Furusaka, M. *Polymer* **1994**, *35*, 2284–2289.
(56) Van Durme, K.; Van Assche, G.; Nies, E.; Van Mele, B. *J. Phys. Chem. B* **2007**, *111*, 1288–1295.
(57) Loozen, E.; Van Durme, K.; Nies, E.; Van Mele, B.; Berghmans, H. *Polymer* **2006**, *47*, 7034–7042.
(58) Bras, W.; Dolbnya, I. P.; Detollenaere, D.; Tol, R.; Malfois, M.; Greaves, G. N.; Ryan, A. J.; Heeley, E. *J. Appl. Crystallogr.* **2003**, *36*, 791–794.
(59) Inorganic Crystal Structure Database, structures for 'hexagonal ice' (Ih) codes: (29065, 64776, 64777). URL: http://www.fiz-karlsruhe.de/icsd.html
(60) Van Durme, K.; Van Assche, G.; Van Mele, B. *Macromolecules* **2004**, *37*, 9596–9605.
(61) Durme, K. V.; Van Mele, B.; Loos, W.; Du Prez, F. E. *Polymer* **2005**, *46*, 9851–9862.
(62) Swier, S.; Pieters, R.; Van Mele, B. *Polymer* **2002**, *43*, 3611–3620.
(63) Van Lokeren, L.; Gotzen, N.; Pieters, R.; Van Assche, G.; Biesemans, M.; Willem, R.; Van Mele, B. *Chem.—Eur. J.* **2009**, *15*, 1177–1185.
(64) Pieters, R. *Phase separation kinetics of aqueous polymer systems by means of modulated temperature DSC*; Vrije Universiteit: Brussels, 2005.
(65) Verjans, W. *Polymeeroplossingen en -mengsels met waterstofbrug interacties*; Katholieke Universiteit: Leuven, 2006.
(66) *Selected powder diffraction data for metals and alloys: data book*; JCPDS--International Centre for Diffraction Data: 1978; Vol. *1*.